Int J Clin Exp Pathol 2016;9(7):6877-6886
www.ijcep.com /ISSN:1936-2625/IJCEP0025457

Original Article

MicroRNA-134 inhibits HCC cell growth and migration through the AKT/GSK3β/SNAIL signaling pathway

Shihai Liu[1,4], Huazheng Pan[2], Jia Cao[3], Ye Liang[1], Xiangping Liu[1], Aihua Sui[1], Liping Wang[1], Quan Zhou[1], Zhaojun Wan[4], Kai Fu[4], Zimin Liu[4], Jun Liang[4]

[1]Department of Medical Research Center, [2]Department of Clinical Laboratory, The Affiliated Hospital of Qingdao University, Qingdao, P. R. China; [3]Clinical Medicine College, Ningxia Medical University, Ningxia, P. R. China; [4]Department of Oncology, Peking University International Hospital, Beijing, P. R. China

Received February 2, 2016; Accepted April 26, 2016; Epub July 1, 2016; Published July 15, 2016

Abstract: MicroRNAs (miRNAs) are a class of small non-coding RNAs that regulate gene expression at both transcriptions and at post-transcriptional level. The present study was to investigate the pathogenic implications of miRNA in hepatocellular carcinoma (HCC) cells and further analyze its characteristics. We found that different expression profiles of miRNAs in tumor and adjacent tissue by miRNA microarray. MiR-134 expression was significantly decreased in human tumors and cancer cells. We demonstrate that miR-134 inhibits cancer cell proliferation, migration and induced apoptosis. Further, GSK3β was identified as a direct target of miR-134, and established the molecular and functional links between miR-134, GSK3β and migration in vitro. We also uncover the molecular pathways through regulating the AKT/GSK3β/SNAIL signaling pathway. Taken together, our findings provide a promising and potential therapeutic target for HCC.

Keywords: HCC, miR-134, migration, GSK3β

Introduction

Hepatocellular carcinoma (HCC) is the sixth most common cancer globally and the second most lethal cancer all over the world [1-3]. Due to the strongest invasion, the fastest metastasis of HCC, HCC is also diagnosed at an advanced stage [4]. Although traditional therapy for the advanced stage of HCC is not very efficient, including surgical resection, transcatheter arterial chemoembolization and liver transplantation, etc, cytotoxic chemotherapy is still the important treatment method [5]. However, metastasis is a significant cause to the high mortality in patients with HCC [6]. The mechanism of metastasis begins when tumor cells break away and grow independently from a primary tumor while migrating through the extracellular matrix. Then, the cells arrested at a distant organ site, micrometastasis formation and metastatic colonization [7, 8]. Each step contributes to intrinsic (i. e., genetic) and extrinsic (i. e., microenvironmental signals) factors. Many molecules involve to this process, and some of these molecules are involved in the mechanical aspects, whereas others regulate signaling pathways [9].

MicroRNAs (miRNAs) are small, endogenous, nonprotein-coding RNA molecules, which bind to complementary sequences in the 3' untranslated region (3' UTR) of multiple target mRNAs. MiRNAs are dysregulated in diverse biological processes, including proliferation, differentiation, development, apoptosis, immunity, and carcinogenesis [10]. This miRNA has been linked to participate in cancer development in humans [11-14]. However, the functions and mechanisms of miRNA-mediated regulation of HCC metastasis or recurrence are largely unknown.

Migration is a key phenotypic characteristic of many cancer cells [15]. MiR-145 was found to positively modulate tumor invasion and metastasis in HCC by acting on the FAK gene [16]. MiR-625 was found to inhibit invasion in HCC cell by downregulating the expression of the IGF2BP1 gene [17]. MiR-331-3p is a miRNA that has been demonstrated to modulate HCC inva-

sion and metastasis by decreasing PH domain and leucine-rich repeat protein phosphatase [18]. By far miRNAs play crucial roles in modulating the invasion and migration of HCC, resulting in changes of cell adhesion, movement and some related adhesion and cytoskeletal molecules, where this is a multistep carcinogenesis process [19].

As a result, we discovered that miR-134 is downregulated in human HCC tissue through the miRNA array and miR-134 acted as a tumor suppressor through inhibiting AKT/GSK3β/SNAIL pathway. These findings provide a framework for better understanding the pathogenesis of HCC.

Materials and methods

Human tissue samples

Frozen tissues from 25 HCC cases were collected from the Department of liver and gall surgery, the Affiliated Hospital of Qingdao University (Qingdao, China) between March 2009 and September 2011. Patients included 20 men and 5 women. The mean ages of the patients at the time of surgery were 53.7 years for men and 53.8 years for women. All patients provided prior consent and approval of the Affiliated Hospital of Qingdao University. The study protocol was approved by the Ethics Committee of the Affiliated Hospital of Qingdao University.

Cell cultures and oligonucleotide transfection

The human HepG2, Hep3B and SMMC7721 HCC cell lines, L02 liver normal cell line, 293 cells were purchased from the Cell Bank Type Culture Collection of the Chinese Academy of Sciences (Shanghai, China). Cells were routinely cultured in DMEM (Hyclone, Thermo Fisher Scientific, Waltham, MA, USA) supplemented with 10% FBS (Gibco, Invitrogen, Carlsbad, CA, USA) at 37°C in a humidified atmosphere of 5% CO_2. For miR-134 overexpression, cells were transfected with 100 nmol/L of miR-134 mimics, which are synthesized by Genepharma (Shanghai, China). For inhibition, cells were transfected with anti-miR-134 (also named miR-134 inhibitors), which are chemically synthesized by Genepharma (Shanghai, China). The sequences were as follows: for miR-134 mimics, 5'-UGUGACUGGUUGACCAGAGGGG-3'; for the negative control oligonucleotide, 5'-CGUCAGU UCCGUTTACGUAACGU-3'; for miR-134 inhibitors, 5'-CCCCUCUGGUCAACCAGUCACA-3'. The entire transfection process was completed using Lipofectamine 2000 (Invitrogen), according to the manufacturer's instructions. Cells were collected 48 h later for migration and western blot assays.

Quantitative RT-PCR (qRT-PCR) analysis of mRNA and miRNA expression

Total RNA from tissues and cells was extracted using RNAiso reagent (Takara Bio Inc., Shiga, Japan) for both mRNA and miRNA analyses. For GSK3β mRNA detection, complementary DNA was synthesized using the PrimeScript RT reagent kit (Takara Bio Inc., Shiga, Japan) and qRT-PCR was performed using SYBR green premix Ex Taq (Takara Bio Inc., Shiga, Japan) and were normalized to levels of GAPDH mRNA. The following primers were used: GSK3β forward, 5'-TGGTCGCCAT CAAGAAAGTATTG-3'; GSK3β reverse, 5'-GCGTCTGTTTGGCTCGACTAT-3'; GAPDH forward, 5'-TCATGGGTGTGAACCATGAGAA-3'; GAPDH reverse, 5'-GGCATGGACTGTGGTCATGAG-3'. For analysis of miR-134 expression, qRT-PCR analyses were carried out using the All-in-One miRNA qRT-PCR Detection Kit (GeneCopoeia, Rockville, MD, USA) according to the manufacturer's instructions (LightCycler 480 II, Roche) and using small nuclear U6 RNA as an internal standard. Relative expression was calculated using the $2^{-\Delta\Delta CT}$ method. All qRT-PCR analyses were carried out in triplicate, and data presented were generated from the means standard errors.

Luciferase reporter assay

HEK 293 cells were plated in 24-well plates at a density of 3×10^4 cells per well. Cells were transfected with 50 ng psiCHECK2 recombination vector and miR-134 mimics or anti-miR-134. Three replicates were made for each transfection. The pRL-TK vector (Promega, Madison, WI, USA) encoding Renilla luciferase was cotransfected as internal control. Relative Firefly and Renilla luciferase activities were evaluated with the Dual-Glo luciferase system (Promega) and measured with a multi-well fluorescence reader (Tecan SAFIRE) at 48 h after transfection. Firefly luciferase activity was normalized to Renilla luciferase activity.

Western blot analysis

Cells were lysed in cell RIPA buffer (Beyotime, Shanghai, China) in the presence of a protease inhibitor cocktail (Sigma Aldrich, Louis, MO, USA), and protein content was quantified by BCA methods. 30 μg total cellular protein was fractionated by 12% (w/v) SDS-PAGE and electronically transferred to 0.45 μm PVDF membrane (Millipore). The membrane was blocked for 2 hours in TBS-Tween 20 (TBST) containing 5% (w/v) non-fat milk, and incubated with primary antibody for 1 h at room temperature. The membrane was washed three times in TBST and incubated with secondary antibody for 1 h. GSK3β was measured by monoclonal anti-GSK3β antibody (Cell Signaling Technology, Danvers, MA). Total and phosphorylation AKT was detected by monoclonal anti- total AKT and phospho-AKT antibody (Cell Signaling Technology, Danvers, MA). Monoclonal anti-SNAIL, anti-GAPDH antibody was used to detect total β-catenin protein. SNAIL was detected by monoclonal SNAIL antibody (Cell Signaling Technology, Danvers, MA). GAPDH protein was used as reference (Cell Signaling Technology, Danvers, MA), and the secondary antibody was HRP-conjugated goat anti-rabbit IgG and HRP-conjugated goat anti-mouse IgG. Membranes were washed and followed by detection and visualization using ECL Western blot detection reagents (Pierce Biotechnology, Rockford, IL).

Cell invasion assay

For the invasion assay, 5×10^4 HepG2 cells were transfected with miR-134 mimics, anti-miR-134 or negative control oligonucleotides, and were placed in the upper chamber of each Matrigel-coated insert (BD Biosciences, Billerica, MA, USA) with a non-coated membrane. Then DMEM containing 10% FBS was added to the lower chamber as a chemoattractant. After incubation at 37°C for several hours, non-migrating cells were removed from the upper part of the insert with cotton swabs. Cells adhering to the lower membrane surface were stained with 0.1% crystal violet in 20% methanol. Cells that had migrated into the lower membrane were manually counted in five randomly chosen fields under a microscope, and photographs were taken using a microscope equipped with an automatic photomicrograph system (Leica, Germany).

Wound healing assay

Wound healing assay was carried out to determine the cell migration ability by transfecting miR-134, anti-miR-134. HepG2 cells were seeded into 6-well dishes and grew until 80%-90% confluence. Sterilized one-milliliter pipette tip was used to generate wounding across the cell monolayer, and the debris was washed with PBS. Migration of cells into the wound was then observed at different time. Cells migrated into the wounded area or protruded from the border of the wound were visualized and photographed under the inverted microscope at the indicated time. A total of ten areas were selected randomly in each well by a 100 × magnification and cells in three wells of each group were quantified in each experiment. The experiment was done in triplicate.

Cell viability assay

Cell viability was assessed by MTT method. Briefly, cells were seeded in 96-well plate at a density of 1×10^4 cells/well. After 24 h incubation, cells were treated with miR-134, anti-miR-134 or the blank vector (mock) was added to the cells while only DMSO (solvent) was added as a blank control. After growing for 24, 48 and 72 h, cells were incubated with MTT (0.5 mg/mL) for 4 h at 37°C. During this incubation period, water-insoluble formazan crystals were formed, which were dissolved by the addition of 100 μL/well DMSO. The optical densities (OD) at 570 nm were measured using an enzyme-linked immunosorbent assay plate reader. Wells containing culture medium and MTT but no cells acted as blanks. Each cell viability assay was performed in quadruplicate and repeated three times.

Statistical analysis

All data were expressed as mean ± standard error of measurement and analyzed using SPSS version 13.0 (SPSS, Chicago, IL, USA), and significance determined with two-tailed Student's t-test. Data were considered statistically significant at $P < 0.05$.

Results

MiR-134 is downregulated in hepatocellular carcinoma

HCC often presents with multiple tumors, with only approximately 25% of tumors originating

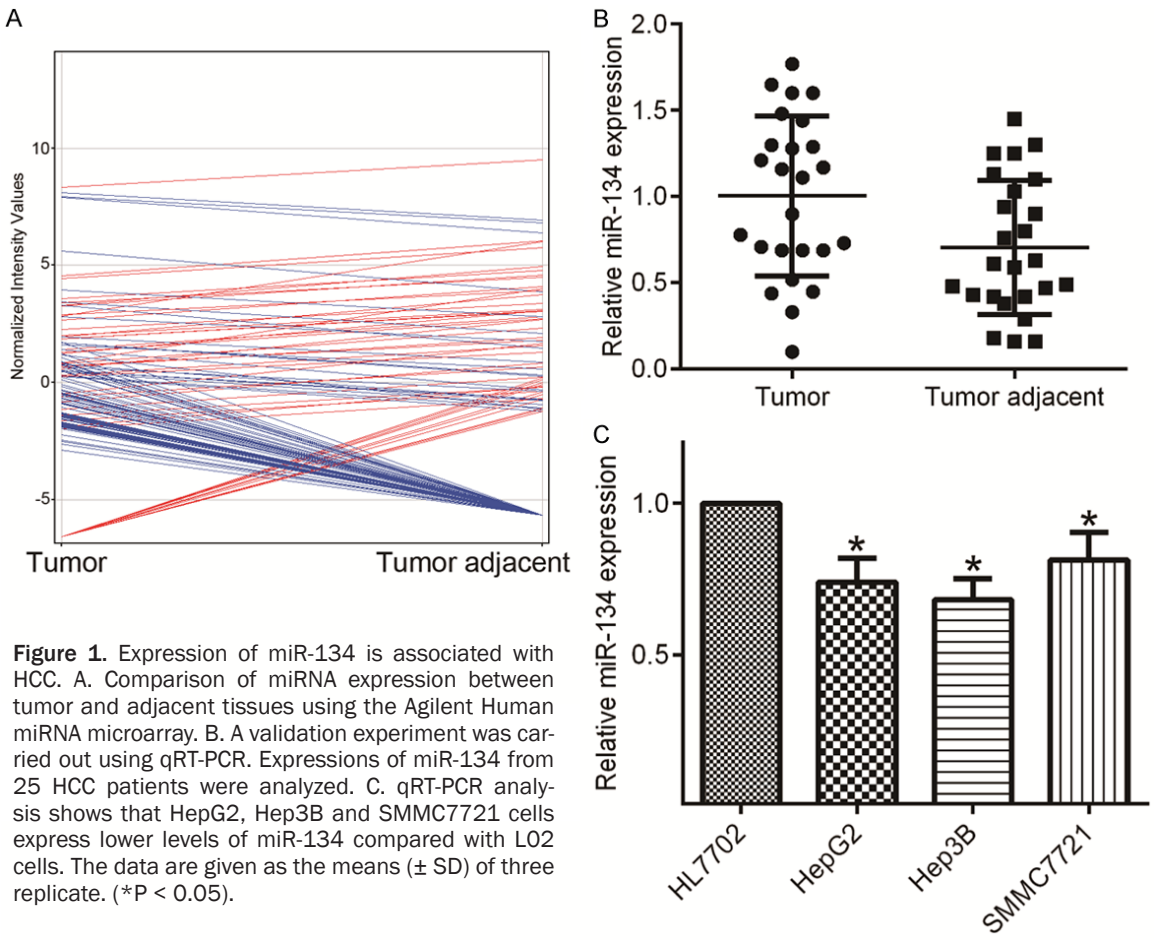

Figure 1. Expression of miR-134 is associated with HCC. A. Comparison of miRNA expression between tumor and adjacent tissues using the Agilent Human miRNA microarray. B. A validation experiment was carried out using qRT-PCR. Expressions of miR-134 from 25 HCC patients were analyzed. C. qRT-PCR analysis shows that HepG2, Hep3B and SMMC7721 cells express lower levels of miR-134 compared with L02 cells. The data are given as the means (± SD) of three replicate. (*P < 0.05).

from de novo lesions. Despite the observation that up to 75% of HCC tumors within a given patient's liver are clonally related, the precise genomic profiles, and therefore likely the phenotypes, are different among tumor and adjacent tissues [20]. Accordingly, we compared miRNA expression profiles between tumor and adjacent tissues of the hepatocellular carcinoma patient by microRNA microarray. The pattern of miRNA expression in tumor tissues was markedly different from the adjacent tissues. After normalization, the expression profiles of 1867 miRNAs were determined between tumor and adjacent tissues, revealing 19 upregulations and 85 downregulations (**Figure 1A**). The most differentially expressed miRNAs were identified and summarized in **Table 1**.

Among the shared 27 significantly decreased miRNAs, we focused on miR-134 because it exhibited more than 40 fold decreased. To further address the relationship between miR-134 and HCC patients, we analyzed miR-134 expression levels in all 25 pairs of HCC tumors and matched tumor adjacent tissues by qRT-PCR (**Figure 1B**). The result was similar to the expression pattern using the miRNA microarray. HepG2, Hep3B and SMMC7721 cell lines, compared with normal liver cell L02, was significanctly downregulated (**Figure 1C**). These results were consistent with the microRNA microarray.

MiR-134 directly targets GSK-3β in human hepatocellular carcinoma cells

To understand the molecular mechanisms by which miR-134 induces tumor profiles, we employed three strategies to identify the potential downstream targets of miR-134: first, we analyzed potential gene targets of miR-134 by prediction algorithms, including miRWalk (http://www.umm.uni-heidelberg.de/apps/zmf/mirwalk), PicTar (http://pictar.mdc-berlin.de/), TargetScan (http://www.targetscan.org) and miRanda (http://www.microrna.org). Among them,

Table 1. Dysregulation of miRNAs in hepatocellular carcinoma tissue

miRNA name	Score (d)
Decreased expression (27)	
hsa-miR-216a-5p	-167.785
hsa-miR-517a-3p	-119.901
hsa-miR-663a	-106.978
hsa-miR-512-3p	-94.4024
hsa-miR-3188	-94.0008
hsa-miR-4465	-92.7766
hsa-miR-642b-3p	-87.0549
hsa-miR-205-3p	-84.4844
hsa-miR-3127-5p	-79.672
hsa-miR-520c-3p	-72.642
hsa-miR-3692-5p	-72.617
hsa-miR-4417	-70.9428
hsa-miR-125a-3p	-59.4713
hsa-miR-10b-5p	-55.1163
hsa-miR-4669	-54.9961
hsa-miR-34a-5p	-53.3617
hsa-miR-34b-5p	-47.7756
hsa-miR-3620-5p	-47.6437
hsa-miR-134	-47.5368
hsa-miR-5187-5p	-45.6114
hsa-miR-202-3p	-45.0858
hsa-miR-5088	-40.6771
hsa-miR-6131	-40.4137
hsa-miR-1181	-40.2024
hsa-miR-4689	-37.5369
hsa-miR-6509-5p	-36.887
hsa-miR-199b-5p	-36.0143
Increased expression (10)	
hsa-miR-557	40.34202
hsa-miR-152	43.19254
hsa-miR-4731-3p	44.37989
hsa-miR-486-5p	58.2291
hsa-miR-483-5p	65.72054
hsa-miR-146a-5p	71.40368
hsa-miR-200b-3p	90.1433
hsa-miR-188-5p	95.2645
hsa-miR-144-3p	101.95
hsa-miR-142-5p	108.7475

GSK-3β was found to be the candidates of miR-134 targets. By analyzing the homology between miR-134 and GSK-3β mRNA sequences, we observed that the 12 nucleotides from the 5' end of miR-134 were complementary to bases 1201-1223 of the GSK-3β cDNA (Homo sapiens, NM_002093; **Figure 2A**). Second, a dual-luciferase reporter assay system was used to validate whether the GSK-3β mRNA transcript is regulated by miR-134 through direct binding to its 3' UTR region of GSK-3β mRNA. As shown in **Figure 2B**, luciferase levels of the miR-134 groups transfected with psi-GSK3β 3UTR WT constructs were significantly decreased, compared to those transfected with psi-GSK3β 3UTR MUT constructs, for the 293 cell line, implying that GSK-3β is a direct target of miR-134. To further demonstrate the correlation between miR-134 and GSK-3β in HepG2 cells, mRNA and protein expression of GSK-3β were detected by qRT-PCR and Western blot. Data showed that miR-134 upregulation dramatically reduced the protein expression of GSK-3β. Meanwhile, we observed that GSK-3β expression was increased by downregulating miR-134 (**Figure 2C-E**). Thus, miR-134 inhibited GSK-3β expression in human hepatocellular carcinoma.

MiR-134 affects the invasion and migration capability in HepG2 cells

Given the low level of miR-134 expression detected in HCC tissues, we asked whether miR-134 may function as a tumor suppressor and could affect cell invasion or migration [24]. To address this question, we transfected miR-134 into HepG2 cells. Transwell assay showed that the invasive speed of HCC cells with highly expressing miR-134 was markedly slower than that of control cells (**Figure 3A** and **3B**). Furthermore, overexpression of miR-134 inhibited wound closure speed of HepG2 cells by wound healing assay (**Figure 3C** and **3D**). These findings suggested that miR-134 could inhibit migration and invasion of HepG2 cells and may function as a tumor suppressor in vitro.

Overexpression of miR-134 inhibited HepG2 cell growth and enhanced apoptosis

The significant reduction of miR-134 expression in HCC cell lines and tissue specimens prompted us to explore the possible biological significance of miR-134 in tumorigenesis. The proliferative ability of HCC cells was determined by MTT assay. The result revealed that miR-134 cells showed a significant reduction in cell viability compared to vector-control or the mock group (**Figure 4A**) (**P < 0.01). We also analyzed the effect of miR-134 on apoptosis in

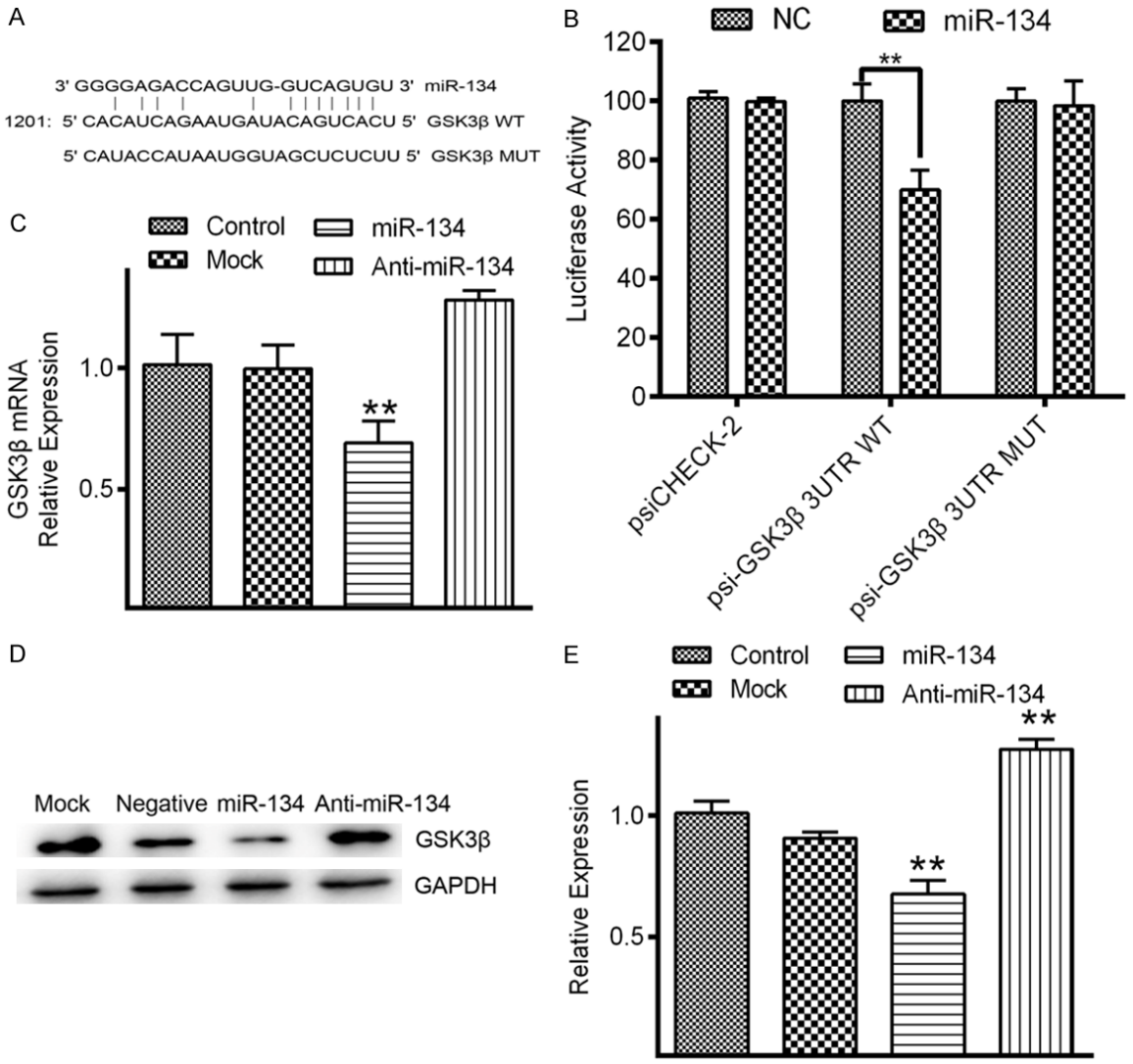

Figure 2. MiR-134 directly targets GSK-3β in HCC. (A) Analyzing the homology of miR-134 and GSK-3β mRNA sequences. The predicted binding site of miR-134 in the 3' UTR of GSK3β. (B) Luciferase assay revealed reduced relative luciferase activities in HEK293 cells following transfection of miR-134 or GSK-3β 3'-UTR, GSK-3β 3'-UTR MUT. (**P < 0.01). (C) GSK3β mRNA measured by qPCR, and (D) protein expression detected by western blot and densitometry analysis (E) in HepG2 at 48 h post-transfection with miR-134 mimics. Data are means of at least three independent experiments; error bars indicate ± SD (*P < 0.05; **P < 0.01).

HCC cells by Annexin V-PI double staining. The Annexin V-positive early-phase apoptotic cells were significantly increased in cells transfected with miR-134 overexpression when compared with untreated or scramble controls cells (**Figure 4B**). Percentages of apoptotic cells are shown in the histogram (**Figure 4C**).

MiR-134 inactivates the Akt/GSK-3β/SNAIL pathway to inhibit HCC migration

Activation of AKT plays an important role in cell migration [21]. We tested the expression of several proteins involved in the Akt/GSK-3β/Snail pathway by western blot analysis and observed that decreased expression of phosphorylated AKT and Snail could be detected in miR-134-transfected cells (**Figure 5A** and **5B**). As expected, opposite expression patterns of these proteins were detected in anti-miR-134 cells (**Figure 5A** and **5B**). Collectively, miR-134 inhibited cell migration through decreasing GSK3β protein translation and phosphorylated AKT, SNAIL level, and the latter inactivated the transcription of genes that repressed cell migration.

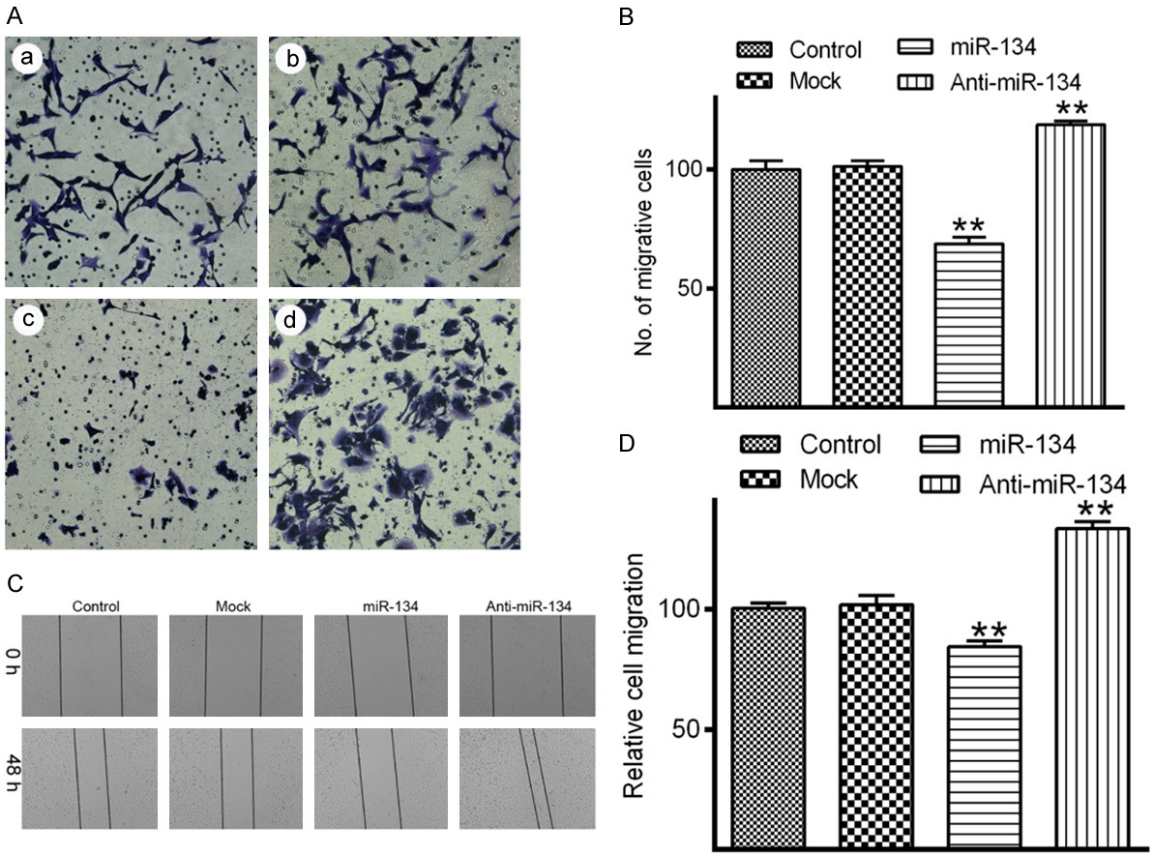

Figure 3. MiR-134 reduces invasion and migration of HCC cells. A, B. Transwell migration system showed that the numbers of migrate cells were significantly reduced compared with the cultures transfected with the negative control oligonucleotide. C. Representative image of scratches from each condition at 0, and 48 h; D. Quantification of wound healing rates. Each bar represents mean values ± SD from three independent experiments. (**P < 0.01).

Discussion

The importance of miRNAs expression in maintaining normal liver cell physiology and HCC gene expression has been well documented [22]. MiR-134 is located at chromosome 14q32.31 [23]. It is worth noting that miR-134 is detected in low expression in ODG and glioblastomas (GBM) [24]. Whereas GSK-3β is upregulated in HCC tissues [25]. However, the association between pathological grade of HCC and miR-134 expression, downregulation of GSK3β expression by miR-134 in HCC cells and knockdown of GSK3β impacting the proliferation and progression of HCC cells are still unclear.

Huang reported that cyclic AMP (cAMP) response element-binding protein (CREB) as a putative target of miR-134 was regulated by miR-134, thereby regulates ischemia/reperfusion injury-induced neuronal cell death [26]. miR-134 could target HSPA12B by binding to its 3'-UTR. miR-134 overexpression promoted neuronal cell death and apoptosis by decreasing HSPA12B protein levels. Conversely, downregulating miR-134 reduced neuronal cell death and apoptosis by enhancing HSPA12B protein levels [27]. MiR-134 inhibits cancer cell and stem-cell proliferation, survival, and xenograft growth, as well as cancer stem-cell self-renewal and stemness through regulation of RTKs MET, EGFR, and PDGF in glioblastoma (GBM) [28]. However, the regulation of miR-134 expression in HCC remains to be elucidated. Moreover, miR-134, miR-487b, and miR-655, which belong to the same cluster located on chromosome 14q32, were associated with EMT in lung adenocarcinoma cells. The miR-134/487b/655 cluster contributed to the TGF-beta1-induced EMT phenomenon and affected the resistance to gefitinib by directly targeting MAGI2, in which suppression subsequently caused loss of PTEN stability in lung cancer

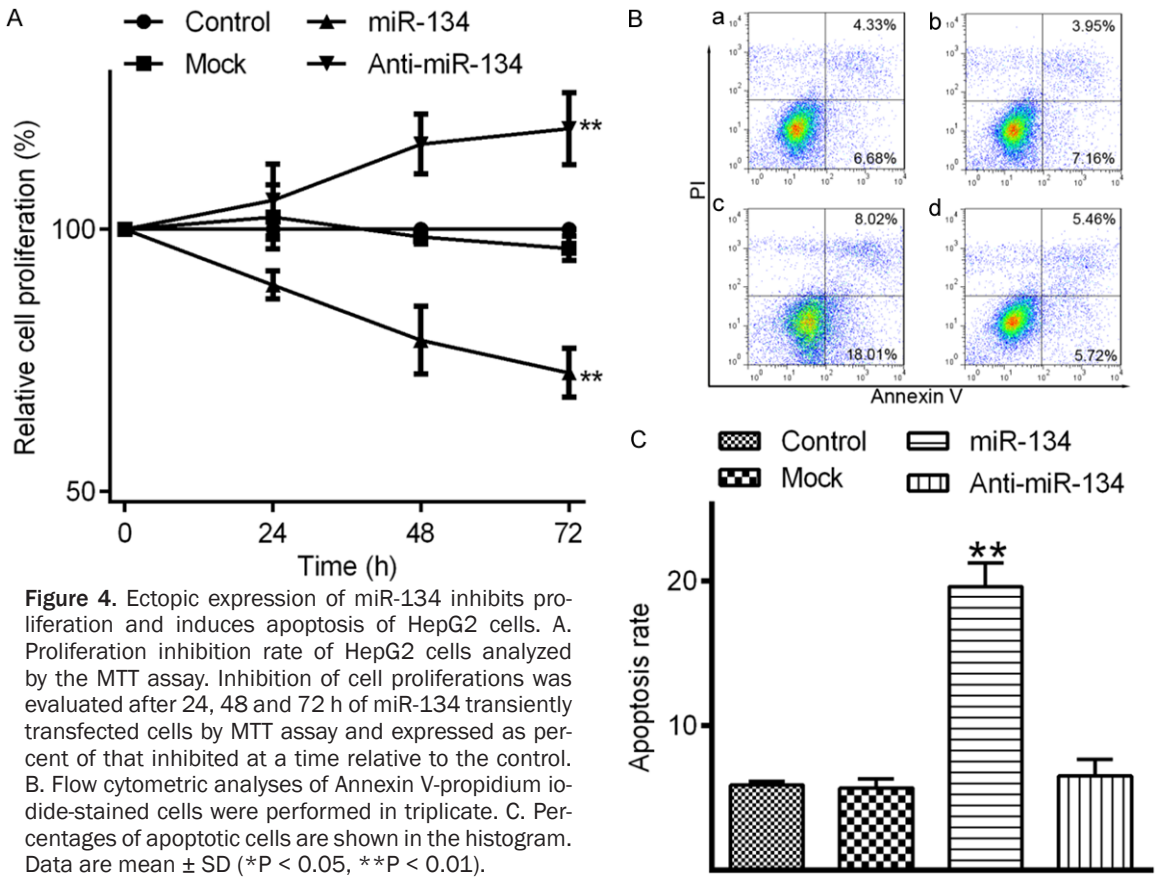

Figure 4. Ectopic expression of miR-134 inhibits proliferation and induces apoptosis of HepG2 cells. A. Proliferation inhibition rate of HepG2 cells analyzed by the MTT assay. Inhibition of cell proliferations was evaluated after 24, 48 and 72 h of miR-134 transiently transfected cells by MTT assay and expressed as percent of that inhibited at a time relative to the control. B. Flow cytometric analyses of Annexin V-propidium iodide-stained cells were performed in triplicate. C. Percentages of apoptotic cells are shown in the histogram. Data are mean ± SD (*P < 0.05, **P < 0.01).

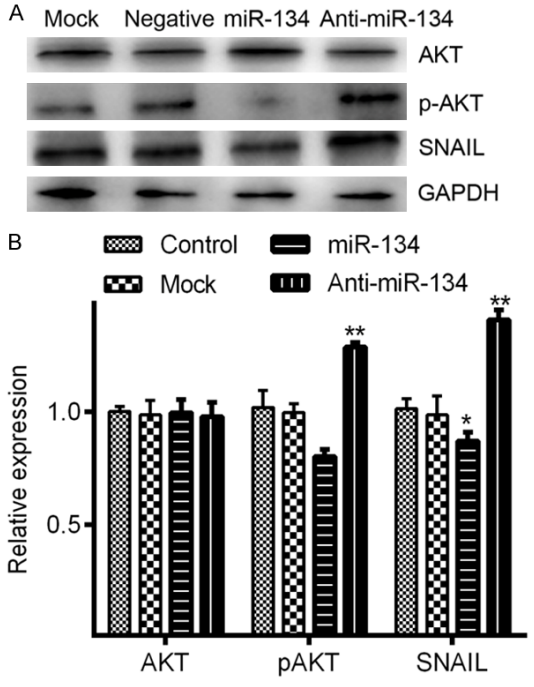

Figure 5. Detection the expression of AKT, p-AKT and SNAIL by transfecting miR-134 or anti-miR-134. After post-transfection with miR-134 or anti-miR-134 into HepG2 cells, western blot (A) detected AKT, p-AKT and SNAIL protein levels, and the differences were analyzed by densitometry analysis (B). Data are means of at least three independent experiments; error bars indicate ± SD (*P < 0.05, **P < 0.01).

cells. The miR-134/miR-487b/miR-655 cluster may be a new therapeutic target in patients with advanced lung adenocarcinoma, depending on the EMT phenomena [29]. Previous work also demonstrated that miR-134 is often downregulated in HCC tissues [30].

Participation of Akt/GSK-3β/snail pathway in the cell migration has also been reported previously in hepatocellular carcinoma line [31, 32]. Further study found that miR-134 was able to decrease the migration of HCC cells via the downregulation of the AKT-GSK3β-Snail signaling pathway. It has been reported that the activation of phosphorylating AKT is able to impact GSK3β activity, ultimately triggering cell migration [33]. Our data indicated that the expression of phosphorylated Akt increased or decreased accordingly when miR-134 was overexpressed or silenced. This change positively correlated with the expression level of GSK-3β and

Snail. Taken together, these results suggest that the role of miR-134 in inhibiting migration was through the inactivation of the AKT-GSK3β-Snail signaling pathway.

In the present study, we investigated the expression of miR-134 in HCC tissues and cells and found that miR-134 was downregulated in HCC and HCC cell line compared to normal liver tissues. It was suggested that miR-134 might be a novel specific biomarker for HCCs. In addition the loss of miR-134 could be involved in HCC development. The miR-134 ectopic expression slowed down tumor cells growth in vitro, compared to vector-control and blank groups. Furthermore, miR-134 overexpression in vitro inhibited migration and invasion in HepG2 HCC cells. We suggest that miR-134 may play a critical role in HCC tumorigenesis and progression. This work suggests that miR-134 could be a novel therapeutic target for the treatment of HCC.

Acknowledgements

This work was supported by grants from the National Natural Science Foundations of China (Grant No. 81372632 and 81402579), the Special Funds of Post doctoral innovation projects of Shandong Province of China (Grant No. 201303063), and the Application of post doctoral funds of Qingdao city, Shandong Province of China (Grant No. 20130118).

Disclosure of conflict of interest

None.

Address correspondence to: Dr. Jun Liang, Department of Oncology, Peking University International Hospital, Life Science Rd., Changping, Beijing 102206, P. R. China. Tel: +86-139-6989-8909; E-mail: liangjun818@126.com

References

[1] Marquardt JU and Thorgeirsson SS. SnapShot: Hepatocellular carcinoma. Cancer Cell 2014; 25: 550, e551.

[2] Dhanasekaran R, Limaye A and Cabrera R. Hepatocellular carcinoma: current trends in worldwide epidemiology, risk factors, diagnosis, and therapeutics. Hepat Med 2012; 4: 19-37.

[3] Gomaa AI, Khan SA, Toledano MB, Waked I and Taylor-Robinson SD. Hepatocellular carcinoma: epidemiology, risk factors and pathogenesis. World J Gastroenterol 2008; 14: 4300-4308.

[4] Zhang B, Shan H, Li D, Li ZR, Zhu KS, Jiang ZB and Huang MS. Cisplatin sensitizes human hepatocellular carcinoma cells, but not hepatocytes and mesenchymal stem cells, to TRAIL within a therapeutic window partially depending on the upregulation of DR5. Oncol Rep 2011; 25: 461-468.

[5] Yang JD and Roberts LR. Hepatocellular carcinoma: A global view. Nat Rev Gastroenterol Hepatol 2010; 7: 448-458.

[6] Liu WC and Liu QY. Molecular mechanisms of gender disparity in hepatitis B virus-associated hepatocellular carcinoma. World J Gastroenterol 2014; 20: 6252-6261.

[7] Honma Y and Harada M. New therapeutic strategy for hepatocellular carcinoma by molecular targeting agents via inhibition of cellular stress defense mechanisms. J UOEH 2014; 36: 229-235.

[8] Valastyan S and Weinberg RA. Tumor metastasis: molecular insights and evolving paradigms. Cell 2011; 147: 275-292.

[9] Zheng T, Yin D, Lu Z, Wang J, Li Y, Chen X, Liang Y, Song X, Qi S, Sun B, Xie C, Meng X, Pan S, Liu J, Jiang H and Liu L. Nutlin-3 overcomes arsenic trioxide resistance and tumor metastasis mediated by mutant p53 in Hepatocellular Carcinoma. Mol Cancer 2014; 13: 133.

[10] Mori M, Triboulet R, Mohseni M, Schlegelmilch K, Shrestha K, Camargo FD and Gregory RI. Hippo signaling regulates microprocessor and links cell-density-dependent miRNA biogenesis to cancer. Cell 2014; 156: 893-906.

[11] Kasuga H, Fukuyama M, Kitazawa A, Kontani K and Katada T. The microRNA miR-235 couples blast-cell quiescence to the nutritional state. Nature 2013; 497: 503-506.

[12] Kumar MS, Armenteros-Monterroso E, East P, Chakravorty P, Matthews N, Winslow MM and Downward J. HMGA2 functions as a competing endogenous RNA to promote lung cancer progression. Nature 2014; 505: 212-217.

[13] Tang D, Shen Y, Wang M, Yang R, Wang Z, Sui A, Jiao W and Wang Y. Identification of plasma microRNAs as novel noninvasive biomarkers for early detection of lung cancer. Eur J Cancer Prev 2013; 22: 540-548.

[14] Mezlini AM, Wang B, Deshwar A, Morris Q and Goldenberg A. Identifying cancer specific functionally relevant miRNAs from gene expression and miRNA-to-gene networks using regularized regression. PLoS One 2013; 8: e73168.

[15] Xia L, Huang W, Tian D, Chen Z, Zhang L, Li Y, Hu H, Liu J, Chen Z, Tang G, Dou J, Sha S, Xu B, Liu C, Ma J, Zhang S, Li M, Fan D, Nie Y and Wu K. ACP5, a direct transcriptional target of FoxM1, promotes tumor metastasis and indi-

cates poor prognosis in hepatocellular carcinoma. Oncogene 2014; 33: 1395-1406.
[16] Luedde T. MicroRNA-151 and its hosting gene FAK (focal adhesion kinase) regulate tumor cell migration and spreading of hepatocellular carcinoma. Hepatology 2010; 52: 1164-1166.
[17] Zhou X, Zhang CZ, Lu SX, Chen GG, Li LZ, Liu LL, Yi C, Fu J, Hu W, Wen JM and Yun JP. miR-625 suppresses tumour migration and invasion by targeting IGF2BP1 in hepatocellular carcinoma. Oncogene 2015; 34: 965-977.
[18] Chang RM, Yang H, Fang F, Xu JF and Yang LY. MicroRNA-331-3p promotes proliferation and metastasis of hepatocellular carcinoma by targeting PH domain and leucine-rich repeat protein phosphatase. Hepatology 2014; 60: 1251-1263.
[19] Ding J, Huang S, Wu S, Zhao Y, Liang L, Yan M, Ge C, Yao J, Chen T, Wan D, Wang H, Gu J, Yao M, Li J, Tu H and He X. Gain of miR-151 on chromosome 8q24.3 facilitates tumour cell migration and spreading through downregulating RhoGDIA. Nat Cell Biol 2010; 12: 390-399.
[20] Chen PJ, Chen DS, Lai MY, Chang MH, Huang GT, Yang PM, Sheu JC, Lee SC, Hsu HC and Sung JL. Clonal origin of recurrent hepatocellular carcinomas. Gastroenterology 1989; 96: 527-529.
[21] Miao H, Li DQ, Mukherjee A, Guo H, Petty A, Cutter J, Basilion JP, Sedor J, Wu J, Danielpour D, Sloan AE, Cohen ML and Wang B. EphA2 mediates ligand-dependent inhibition and ligand-independent promotion of cell migration and invasion via a reciprocal regulatory loop with Akt. Cancer Cell 2009; 16: 9-20.
[22] Zhou JN, Zeng Q, Wang HY, Zhang B, Li ST, Nan X, Cao N, Fu CJ, Yan XL, Jia YL, Wang JX, Zhao AH, Li ZW, Li YH, Xie XY, Zhang XM, Dong Y, Xu YC, He LJ, Yue W and Pei XT. MicroRNA-125b attenuates epithelial-mesenchymal transitions and targets stem-like liver cancer cells through small mothers against decapentaplegic 2 and 4. Hepatology 2015; 62: 801-815.
[23] Fiore R, Khudayberdiev S, Christensen M, Siegel G, Flavell SW, Kim TK, Greenberg ME and Schratt G. Mef2-mediated transcription of the miR379-410 cluster regulates activity-dependent dendritogenesis by fine-tuning Pumilio2 protein levels. EMBO J 2009; 28: 697-710.
[24] Lages E, Guttin A, El Atifi M, Ramus C, Ipas H, Dupre I, Rolland D, Salon C, Godfraind C, deFraipont F, Dhobb M, Pelletier L, Wion D, Gay E, Berger F and Issartel JP. MicroRNA and target protein patterns reveal physiopathological features of glioma subtypes. PLoS One 2011; 6: e20600.
[25] Qiao G, Le Y, Li J, Wang L and Shen F. Glycogen synthase kinase-3beta is associated with the prognosis of hepatocellular carcinoma and may mediate the influence of type 2 diabetes mellitus on hepatocellular carcinoma. PLoS One 2014; 9: e105624.
[26] Huang W, Liu X, Cao J, Meng F, Li M, Chen B and Zhang J. miR-134 regulates ischemia/reperfusion injury-induced neuronal cell death by regulating CREB signaling. J Mol Neurosci 2015; 55: 821-829.
[27] Chi W, Meng F, Li Y, Li P, Wang G, Cheng H, Han S and Li J. Impact of microRNA-134 on neural cell survival against ischemic injury in primary cultured neuronal cells and mouse brain with ischemic stroke by targeting HSPA12B. Brain Res 2014; 1592: 22-33.
[28] Zhang Y, Kim J, Mueller AC, Dey B, Yang Y, Lee DH, Hachmann J, Finderle S, Park DM, Christensen J, Schiff D, Purow B, Dutta A and Abounader R. Multiple receptor tyrosine kinases converge on microRNA-134 to control KRAS, STAT5B, and glioblastoma. Cell Death Differ 2014; 21: 720-734.
[29] Kitamura K, Seike M, Okano T, Matsuda K, Miyanaga A, Mizutani H, Noro R, Minegishi Y, Kubota K and Gemma A. MiR-134/487b/655 cluster regulates TGF-beta-induced epithelial-mesenchymal transition and drug resistance to gefitinib by targeting MAGI2 in lung adenocarcinoma cells. Mol Cancer Ther 2014; 13: 444-453.
[30] Yin C, Wang PQ, Xu WP, Yang Y, Zhang Q, Ning BF, Zhang PP, Zhou WP, Xie WF, Chen WS and Zhang X. Hepatocyte nuclear factor-4alpha reverses malignancy of hepatocellular carcinoma through regulating miR-134 in the DLK1-DIO3 region. Hepatology 2013; 58: 1964-1976.
[31] Assinder SJ, Dong Q, Kovacevic Z and Richardson DR. The TGF-beta, PI3K/Akt and PTEN pathways: established and proposed biochemical integration in prostate cancer. Biochem J 2009; 417: 411-421.
[32] Wu J, Ru NY, Zhang Y, Li Y, Wei D, Ren Z, Huang XF, Chen ZN and Bian H. HAb18G/CD147 promotes epithelial-mesenchymal transition through TGF-beta signaling and is transcriptionally regulated by Slug. Oncogene 2011; 30: 4410-4427.
[33] Cohen P and Frame S. The renaissance of GSK3. Nat Rev Mol Cell Biol 2001; 2: 769-776.